nature physics

SUPPLEMENTARY INFORMATION

https://doi.org/10.1038/s41567-017-0022-7

In the format provided by the authors and unedited.

Critical regimes driven by recurrent mobility patterns of reaction–diffusion processes in networks

J. Gómez-Gardeñes[1,2]*, D. Soriano-Paños[2] and A. Arenas[3]*

[1]GOTHAM Lab, Institute for Biocomputation and Physics of Complex Systems (BIFI), University of Zaragoza, Zaragoza, Spain. [2]Department of Condensed Matter Physics, University of Zaragoza, Zaragoza, Spain. [3]Departament d'Enginyeria Informàtica i Matemàtiques, Universitat Rovira i Virgili, Tarragona, Spain. *e-mail: gardenes@gmail.com; alexandre.arenas@urv.cat

Supplementary Information: Critical regimes driven by recurrent mobility patterns of reaction-diffusion processes in networks

J. Gómez-Gardeñes[1,2], D. Soriano-Paños[2], A. Arenas[3*]

[1]*Institute for Biocomputation and Physics of Complex Systems (BIFI), University of Zaragoza, 50018 Zaragoza, Spain*

[2]*Department of Condensed Matter Physics, University of Zaragoza, 50009 Zaragoza, Spain*

[3]*Departament d'Enginyeria Informàtica i Matemàtiques, Universitat Rovira i Virgili, 43007 Tarragona, Spain*

Corresponding authors: gardenes@gmail.com, alexandre.arenas@urv.cat

1 Linearisation of the Markovian equations

To analyze the steady state of the dynamics, near to the critical point, we linearise Eq. (5) of the main text:

$$\mu\rho_i^* = (1-\rho_i^*)\Pi_i \ , \tag{1}$$

where ρ_i^* is the stationary density of infected individuals associated to node i and

$$\Pi_i = (1-p_d)\left(1-\prod_{j=1}^{N}(1-\lambda\rho_j^*)^{n_{j\to i}}\right) + p_d\sum_{j=1}^{N}\frac{W_{ij}}{\sum_l W_{il}}\left(1-\prod_{l=1}^{N}(1-\lambda\rho_l^*)^{n_{l\to j}}\right) \ . \tag{2}$$

Close to the critical point the disease becomes endemic and $\rho_i^* = \epsilon_i^* << 1 \ \forall \ i$. Therefore,

we can neglect second order terms in ϵ in the above expression and linearise:

$$\Pi_i \simeq (1-p_d)\sum_{j=1}^{N}\lambda\epsilon_j^* n_{j\to i} + p_d\sum_{j=1}^{N}\frac{W_{ij}}{\sum_l W_{il}}\sum_{l=1}^{N}\lambda\epsilon_j^* n_{l\to j} \ . \tag{3}$$

Recalling the expression for $n_{j\to i}$:

$$n_{j\to i} = \delta_{ij}(1-p_d)n_i + p_d\frac{W_{ji}}{\sum_{l=1}^{N} W_{jl}}n_j \ ,$$

and substituting in Eq. (3):

$$\begin{aligned}
\Pi_i &\simeq (1-p_d)\sum_{j=1}^{N}\lambda\epsilon_j^*\left[(1-p_d)\delta_{ij}n_j + p_d\frac{W_{ji}}{\sum_l w_{jl}}n_j\right] + \\
&+ p_d\sum_{j=1}^{N}\frac{W_{ij}}{\sum_l w_{il}}\left(\sum_{l=1}^{N}\lambda\epsilon_l^*\left[(1-p_d)\delta_{jl}n_l + p_d\frac{W_{lj}}{\sum_k w_{lk}}n_l\right]\right) = \\
&= \lambda\sum_{j=1}^{N}\left[(1-p_d)^2\epsilon_j^*\delta_{ij}n_j + p_d(1-p_d)\epsilon_j^* n_j\left(\frac{W_{ij}}{s_i}+\frac{W_{ji}}{s_j}\right)\right] + \\
&+ \lambda p_d^2\sum_{j=1}^{N}\sum_{l=1}^{N}\epsilon_l^* n_l\frac{W_{ij}}{s_i}\frac{W_{lj}}{s_l} \ ,
\end{aligned} \tag{4}$$

where $s_i = \sum_j W_{ij}$ and the following equality $\sum_l \epsilon_l n_l \delta_{jl} = n_j\epsilon_j$ has been used. Defining the row-stochastic matrix $\mathbf{R}$ as:

$$R_{ij} = \frac{W_{ij}}{s_i} \ , \tag{5}$$

we can write Eq. (4) as:

$$\Pi_i = \lambda\sum_{j=1}^{N}\underbrace{\left[(1-p_d)^2\delta_{ij}n_j + p_d(1-p_d)n_j\left(\mathbf{R}+\mathbf{R^T}\right)_{ij} + p_d^2 n_j\left(\mathbf{R}\cdot\mathbf{R^T}\right)_{ij}\right]}_{M_{ij}}\epsilon_j^* = \lambda\left(\mathbf{M}\vec{\epsilon^*}\right)_i \ . \tag{6}$$

Finally, substituting Eq. (6) in Eq. (1), and keeping up to first order in ϵ_i, we obtain:

$$\frac{\mu}{\lambda}\epsilon_i^* = \left(\mathbf{M}\vec{\epsilon^*}\right)_i \ , \tag{7}$$

that defines an eigenvalue problem and thus the epidemic threshold λ_c (the minimum λ value so that the above expression holds) is related to the maximum eigenvalue Λ_{max} of matrix $\mathbf{M}$ as:

$$\lambda_c = \frac{\mu}{\Lambda_{\max}(\mathbf{M})} \ . \tag{8}$$

2 Perturbative approach to evaluate the epidemic threshold

The analytical expression of the epidemic threshold, Eq. (8) demands the knowledge of the maximum eigenvalue of matrix $\mathbf{M}$. Unfortunately, it is not possible to obtain an exact expression for this maximum eigenvalue for any general matrix M and then one has to rely on numerical diagonalisation techniques to obtain λ_c. On the other hand, we can obtain some intuition about the way λ_c behaves close to $p_d = 0$ making use of perturbation theory [1]. To this aim, we consider the terms of matrix elements M_{ij} up to first order in p_d:

$$M_{ij} \simeq \delta_{ij} n_j + p_d \cdot n_j (R_{ij} + R_{ji} - 2\delta_{ij}) \; . \tag{9}$$

We now write the eigenvalues of $\mathbf{M}$ as follows:

$$\lambda_i \;\; = \;\; \lambda_i^{(0)} + p_d \lambda_i^{(1)} + p_d^2 \lambda_i^{(2)} \; . \tag{10}$$

Since the unperturbed ($p_d = 0$) matrix is diagonal, its eigenvalues $\{\lambda_i^{(0)}\}$ correspond to the population of each node and its eigenvectors ($\mathbf{x_1}$, $\mathbf{x_2}$, ..., $\mathbf{x_N}$) are the canonical basis of $\mathcal{R}^N$, ($\mathbf{e_1}$, $\mathbf{e_2}$, ..., $\mathbf{e_N}$), where N is the number of patches of the metapopulation. Since matrix $\mathbf{M}$ is in general not symmetric, we also require the eigenvectors of the transposed matrix, ($\mathbf{y_1}$, $\mathbf{y_2}$, ..., $\mathbf{y_N}$), that for the unperturbed case are again the canonical basis ($\mathbf{e_1}$, $\mathbf{e_2}$, ..., $\mathbf{e_N}$).

Now we consider the terms of the matrix perturbation $M'_{ij} = n_j(R_{ij} + R_{ji} - 2\delta_{ij})$. This way, following [1], we can calculate the correction of the eigenvalues $\lambda_i^{(1)}$ and $\lambda_i^{(2)}$ as:

$$\lambda_i^{(1)} \;\; = \;\; \mathbf{y_i}^T \mathbf{M'} \mathbf{x_i} = M'_{ii} = 2n_i(R_{ii} - 1) \; , \tag{11}$$

$$\begin{aligned} \lambda_i^{(2)} \;\; &= \;\; \sum_{j \neq i} \frac{(\mathbf{y_i}^T \mathbf{M'} \mathbf{x_j})(\mathbf{y_j}^T \mathbf{M'} \mathbf{x_i})}{\lambda_i^0 - \lambda_j^0} = \sum_{j \neq i} \frac{M'_{ij} M'_{ji}}{n_i - n_j} = \\ &= \;\; \sum_{j \neq i} \frac{n_j n_i (R_{ij} + R_{ji} - 2\delta_{ij})^2}{n_i - n_j} = \sum_{j \neq i} \frac{n_j n_i (R_{ij} + R_{ji})^2}{n_i - n_j} \; . \end{aligned} \tag{12}$$

Finally, the eigenvalues of $\mathbf{M}$ close to $p_d = 0$ can be estimated from Eqs.(11) and (12) as:

$$\lambda_i \approx n_i + 2p_d n_i (R_{ii} - 1) + p_d^2 \sum_{j \neq i} \frac{n_j n_i (R_{ij} + R_{ji})^2}{n_i - n_j} \tag{13}$$

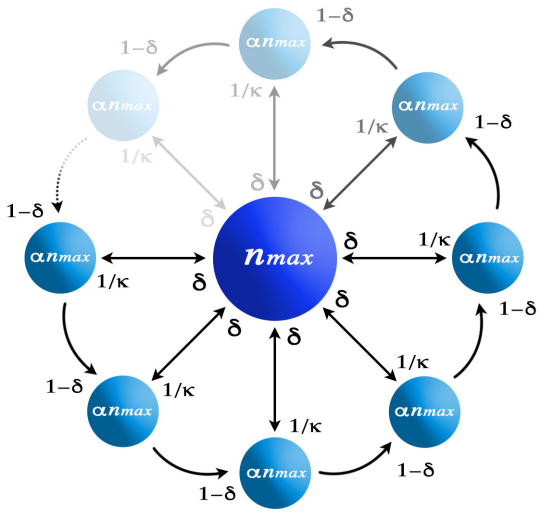

Figure 1: Schematic representation of the star-like network used, whose relevant parameters are α (relating the populations of the hub and each leave), δ indicating the probability that an agent associated to a leave moves to the hub, and k the number of leaves surrounding the hub.

3 Analytical estimation of epidemic threshold dependence on the agents mobility in a toy-model network.

Here we show the estimation of the borders between regions I, II and III as a result of using perturbation theory to derive the maximum eigenvalue of matrix M close to $p_d = 0$. As shown in the main text, according to the perturbation theory p_d^* can be written as:

$$p_d^* = \frac{1 - R_{max,max}}{\sum_{j \neq max} \frac{n_j (R_{max,j} + R_{j,max})^2}{n_{max} - n_j}} \, . \tag{14}$$

This expression, considering the topology of the star-like metapopulation, reads:

$$p_d^* = \frac{1 - \alpha}{k\alpha \left(\frac{1}{k} + \delta\right)^2} \, , \tag{15}$$

that can be re-written as:

$$\alpha = \frac{1}{1 + p_d^* \left(\frac{1}{k} + 2\delta + k\delta^2\right)} \, . \tag{16}$$

Eq.(16) allows us to estimate the border between the three possible regimes. Indeed, the border between critical behaviors I and II is given by setting $p_d^* = \frac{1}{n_{max}}$, whereas the border between regions II and III is obtained when $p_d^* = 1$. These limits are represented in Fig. 2 by dashed white lines, showing a good agreement with the analytical solutions when $\delta > k^{-1}$. This limit is due

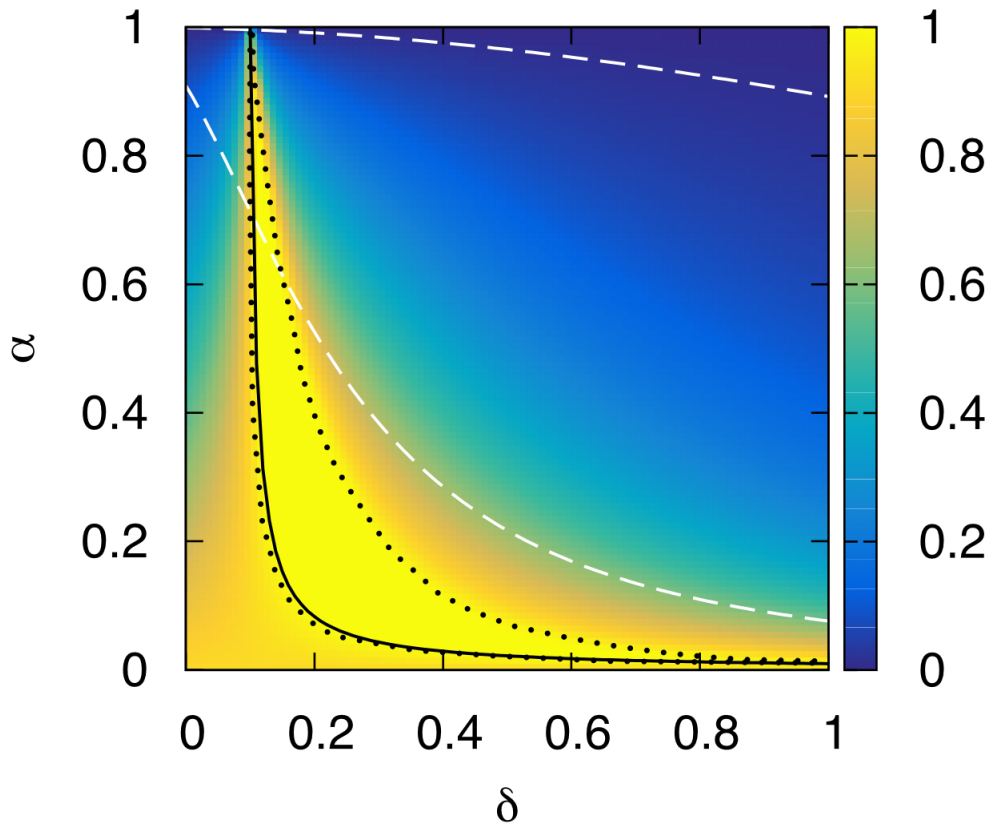

Figure 2: Representation of the value of the mobility for which the epidemic threshold reaches its maximum (p_d^*) as a function of (δ, α). The dotted lines highlight the border between regions II and III (for which epidemic detriment occurs in the whole range $p_d \in [0, 1]$). Estimations of the border of each regimen by using Eq.(16) are shown by dashed white lines, whereas the solid black curve is the prediction for $p_d^* = 1$ obtained with the function $\alpha(\delta)$, Eq. (21), derived from the heuristic explanation of epidemic detriment.

to the assumption made when implementing the perturbative approach, namely that the hub is the most populated node. This assumption, when $\delta < k^{-1}$ is not ensured for any pair of values (p_d, α) since periphery nodes (leaves) become more populated than the hub.

4 Heuristic explanation of spreading detriment

Let us start by writing the effective population of the hub in the star-like metapopulation:

$$n_h^{eff}(p_d) = \sum_j n^{j\to h} = n_{max}(1-p_d) + p_d k\alpha n_{max}\delta \ , \tag{17}$$

while that for a leave reads:

$$n_l^{eff}(p_d) = \alpha n_{max}(1-p_d) + p_d\alpha n_{max}(1-\delta) + p_d n_{max}\frac{1}{k} \ . \tag{18}$$

Our insight is that the epidemic detriment is due to the fact that the effective populations of the leaves and the hub tend to become similar as p_d increases. Thus, being $n_h^{eff}(p_d)$ and $n_h^{eff}(p_d)$ linear functions of p_d and considering that $0 < \alpha < 1$, for this to happen it is necessary that:

$$\frac{\mathrm{d}n_h^{eff}}{\mathrm{d}p_d} = n_{max}(k\alpha\delta - 1) < 0 \ , \tag{19}$$

$$\frac{\mathrm{d}n_l^{eff}}{\mathrm{d}p_d} = \frac{n_{max}}{k}(1 - k\alpha\delta) > 0 \ . \tag{20}$$

These two conditions are satisfied when $\alpha < (k\delta)^{-1}$. This expression gives us a limit, which is represented with a black dashed line in Figure 1.c in the main text, for this intuitive argument. Given this condition, if the two derivatives are very small (in modulus) then the effective population of the hub will keep approaching to that of each leave for the whole range $p_d \in [0, 1]$. To obtain an estimation of the border between region II and III we now consider that the value of p_d for which the two effective populations are equal is $p_d = 1$. This way we obtain the following curve:

$$\alpha = \frac{1}{k^2\delta - k(1-\delta)} \ , \tag{21}$$

whose shape is the solid black curve plotted in Fig. 2.

Beyond $\alpha = (k\delta)^{-1}$, it is mandatory to make a more restrictive argument in order to explain the detriment, since effective populations are no longer homogenising. At this point, let us recall that recovery processes play an important role because, without recovery, the incidence of the disease scale up the whole population for any value of λ. Besides, although more agents contacts inside the hub in this scenario, leaves are emptier while increasing the mobility. This fact turns the leaves into places where contagion processes barely take place, so that they behave as recovery places. This way, for small values of mobility, the increase of contagion processes can not compensate the recovery ones, leading to a detriment of the epidemic. If this condition is fulfilled, the epidemic threshold for small values of the mobility will be determined by the individuals who do not leave the hub so that this threshold will be larger with the mobility (recall that the threshold is proportional to N^{-1}).

To characterise this balance between recovery and contagion, let us measure the evolution of the impact of a disease after imposing its initial seed. For this purpose, we have used the basic reproductive number R_0, which indicates the number of contagions caused by an initial infected seed during the period it remains contagious. In our case, i.e, a well-mixed population of n_i^{eff} inside each node, this parameter is given by:

$$(R_0)_i = \frac{\lambda n_i^{eff}(p_d)}{\mu} \, , \tag{22}$$

where i represents the hub or any leaf. To justify the detriment, let us assume that contagion rate corresponds to the epidemic threshold in the static case, so that $\lambda = \mu/n_{max}$. Besides, we suppose that a fraction of x agents associated to each node are initially infected, with $x << 1$. Under these premises, given a value of the mobility p_d, the number of new infected people I_i^n from the initial seed can be computed as:

$$I_h^n = (R_0)_h I_h^{eff} \, , \tag{23}$$

$$I_l^n = (R_0)_l I_l^{eff} \, , \tag{24}$$

where I_h^{eff} and I_l^{eff} denote the effective number of infected agents inside the hub and leaf respectively. Assuming that these values correspond to the initial situation, the number of new infected individuals can be computed as:

$$I_h^n = \frac{\left(n_h^{eff}(p_d)\right)^2}{n_{max}} x \,, \tag{25}$$

$$I_l^n = \frac{\left(n_l^{eff}(p_d)\right)^2}{n_{max}} x \,. \tag{26}$$

For the sake of simplicity, we will make this argument with the star network, i.e., imposing $\delta = 1$. Using Eqs. (17,18), the previous expressions read:

$$I_h^n = n_{max} x \left[1 + p_d \left(k\alpha - 1\right)\right]^2 , \tag{27}$$

$$I_l^n = n_{max} x \left[\alpha + p_d \left(1/k - \alpha\right)\right]^2 \,. \tag{28}$$

Therefore, the total number of infected people I from the initial seed is given by:

$$I = I_h^n + k I_l^n = n_{max} x \left\{\left[1 + p_d \left(k\alpha - 1\right)\right]^2 + k \left[\alpha + p_d \left(1/k - \alpha\right)\right]^2\right\} . \tag{29}$$

Our intuition is that, given a value of p_d, if this quantity is lower than the initial number of infected people, i.e, $I < n_{max} x \left(1 + k\alpha\right)$ we can observe epidemic detriment since the number of infected people will progressively decrease to zero. To support this statement, in Figure 3 we represent I as a function of the agents mobility p_d for several values of the asymmetry along with the mobility dependence of the epidemic threshold. As we can notice there, the equation $I = n_{max} x \left(1 + k\alpha\right)$ gives us a good estimation about the detriment zone with respect to the static case. Moreover, it is clear that when there is no population asymmetry, i.e, when $\alpha = 1$ epidemic detriment is not possible since the epidemic size grows with respect to its seed for any value of the agents mobility p_d.

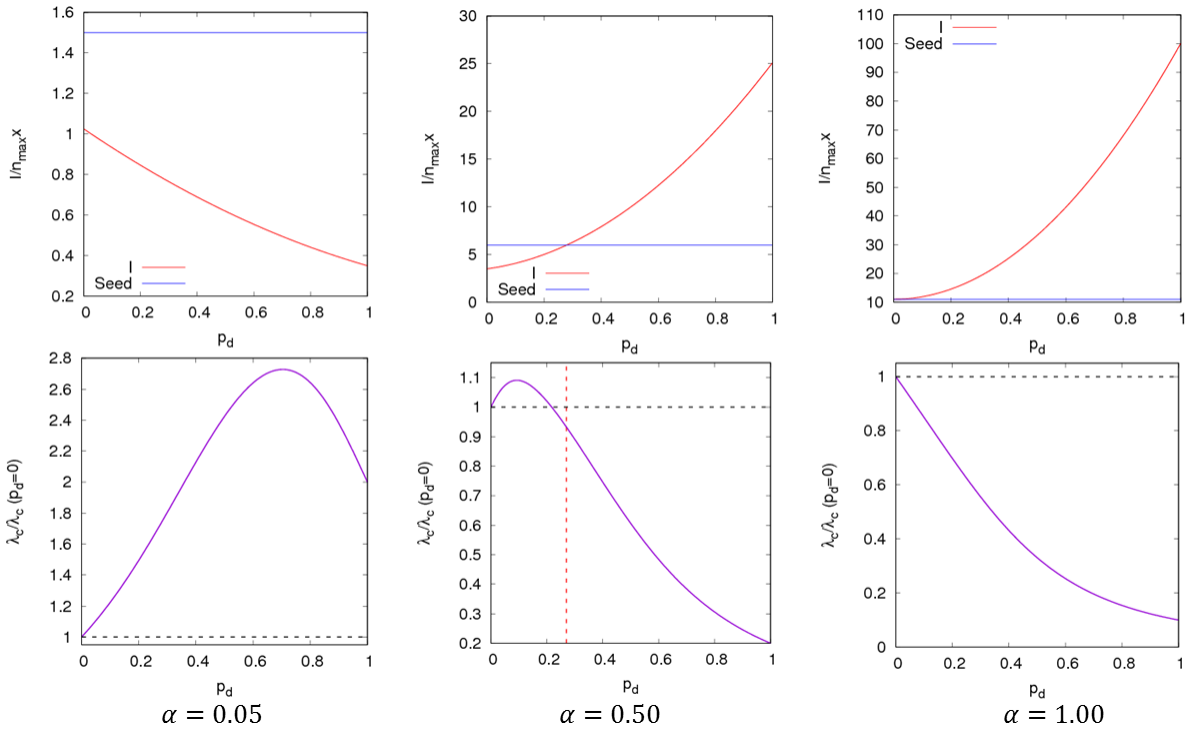

Figure 3: Top: Infected agents from the initial agents in function of p (red lines). Blue lines show the number of agents who are initially infected. Bottom: Mobility dependence of the epidemic threshold (purple lines). Red dashed line indicates the solution for $I = n_{max}x\,(1 + k\alpha)$ whereas black dashed lines show us the value of the epidemic threshold in the static case, i.e, for $p_d = 0$. From left to right, the values of asymmetry which have been introduced are $\alpha = 0.05$, $\alpha = 0.5$ and $\alpha = 1.0$.

5 Spatio-temporal epidemic dynamics

To show the microscopical processes which lead to the epidemic detriment, we have performed Monte Carlo simulations in which we monitor the temporal evolution of the epidemic size inside the hub and a leaf. For the sake of comparison, in these simulations we have considered the contagion probability λ to be equal to the epidemic threshold for the static case: $\lambda = \mu/n_{max}$.

Besides, the simulations are carried out for a case where there is a homogenisation in terms of effective populations with the mobility ($\alpha < (\delta k)^{-1}$) as well as for a case in which asymmetry of effective populations become larger with the mobility ($\alpha > (\delta k)^{-1}$).

Results of these simulations are shown in Fig.4. Concretely, Fig.4.a contains the temporal evolution of the disease spreading across a star metapopulation ($\delta = 1$) with $\alpha = 0.05$ and $p_d = 0.1$. It is clear that the homogenisation of the populations leads to a monotonous decrease of the epidemic size inside the hub, since the effective number of contacts per agent decrease so that the contagion rate is not large enough to hold the epidemic. Besides, although agents from the leaves contact with more agents than in the static case, the number of infected agents from the leaves decreases since these contacts are lower than the number of contacts inside the hub in the static case.

On the other hand, Fig.4.b shows the temporal evolution of a disease using another star-like network with $\alpha = 0.4$ and $p_d = 0.1$. In this case, since the effective population as well as the effective number of infected agents inside hub increases with the mobility, the number of infected agents associated to the hub also initially grows. However, leaves empty with mobility so that more agents from there recover than become infected, leading to a decrease of the number of infected agents associated to the leaves. After some time steps, although the effective population inside the hub is larger than in the static case, a homogenisation in terms of infected people takes place because of the small number of infected individuals who move from the leaves to the hub. This homogenisation leads to an epidemic detriment, as we have explained in the previous sections, since contagion processes can not compensate the recovery ones.

We have also included in Figure 4.c the case in which there is no asymmetry in population, i.e, $\alpha = 1$. As we can notice there, detriment does not occur since the number of infected agents from the hub as well as from leaves increase from the initial seed to get a non-zero value.

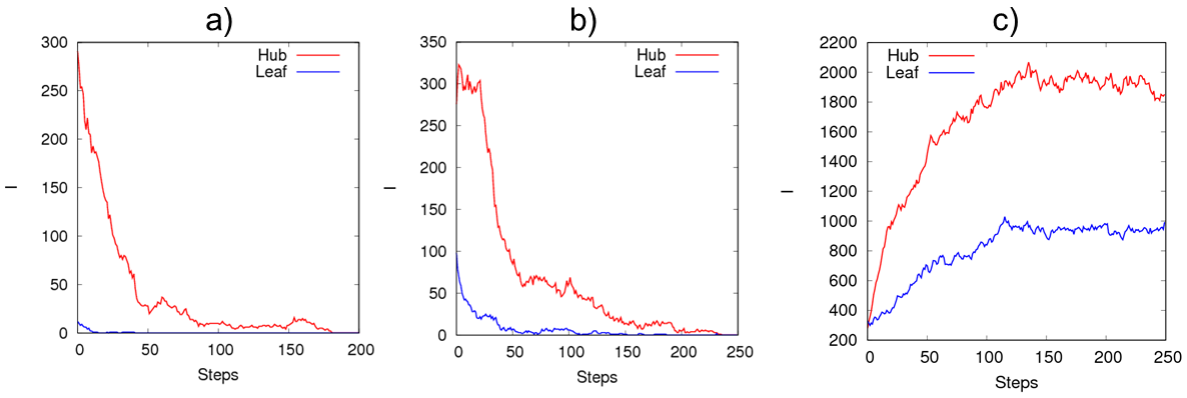

Figure 4: Temporal evolution of the number of infected agents associated to the hub (blue) and to a leaf (red) by starting with a seed composed by the 3% of the whole population. For both cases, the agents mobility p_d and the recovery rate μ are set to $(p_d, \mu) = (0.1, 0.2)$. The networks which have been used are star-like networks ($\delta = 1$) with $k = 10$. The population of the hub is set to $n_{max} = 10000$, whereas the introduced asymmetries are respectively $\alpha = 0.05$ (a), $\alpha = 0.4$ (b) and $\alpha = 1$ (c).

At this point, to further illustrate the validity of the microscopic Markovian equations, we analyze the spatio-temporal evolution of the epidemic incidence when a single subpopulation is initially infected and compare with the results obtained through Montecarlo simulations. In particular, considering the real metapopulation of the city of Cali (Fig. 5.a) we start by infecting a small amount of agents associated to patch 20 and then monitor the time evolution of the contagion across the different 22 patches composing the system. This way, we can also check the different invasion patterns of an epidemic whose seed is spatially localised.

In Fig. 5.b we show the pattern $\rho_i(t)$ as obtained from the Monte Carlo simulation. It becomes clear that contagions remain localized in node 20 for a transient time before initiating a cascade of infections $20 \rightarrow 6 \rightarrow 13 \rightarrow 5, 11, 15 \rightarrow$ ... (see highlighted links in Fig.5.a before

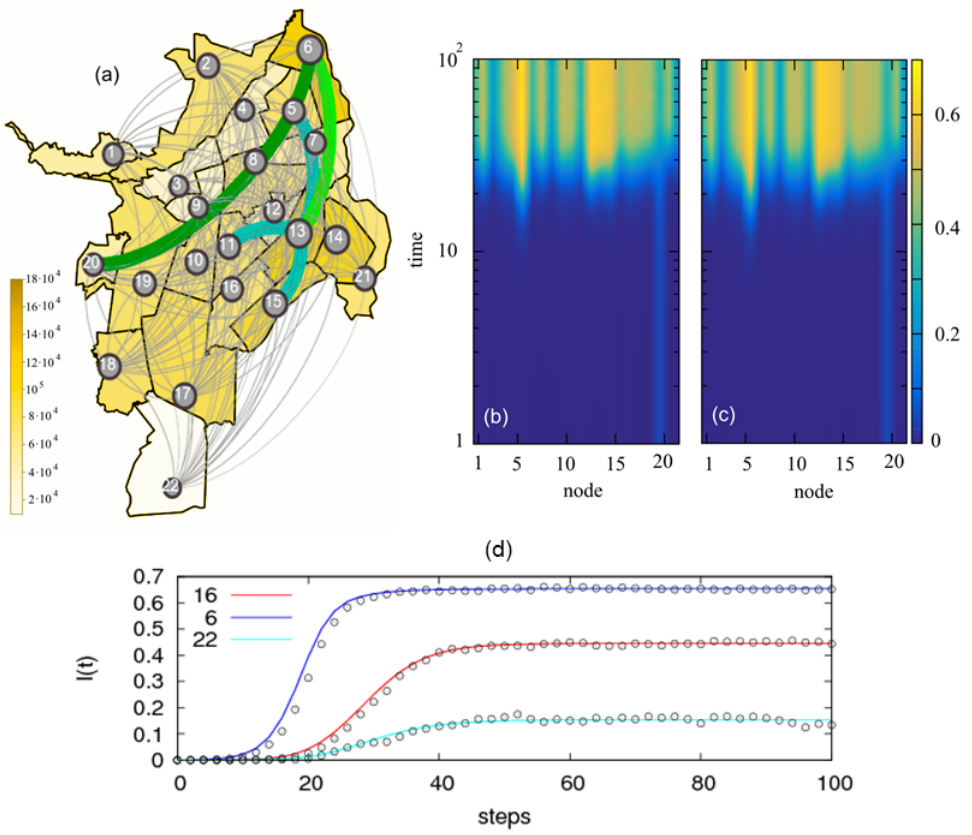

Figure 5: In **(a)** we show the metapopulation of Cali (Colombia) with the commuting network connecting the 22 patches. The color code of each district indicates its population. Panels **(b)** and **(c)** show the spatio-temporal evolution of the epidemic incidence when a single subpopulation (subpopulation 20) is initially infected. The results shown are obtained from Monte Carlo simulations **(b)** and by solving the microscopic Markovian model **(c)**. In **(d)** we show the temporal evolution of the fraction of infected agents in neighbourhoods 6, 16 and 22 as predicted by the Markovian model (solid lines) and as obtained from MC simulations (dots). The value of the recovery probability is set to $\mu = 0.2$, whereas contagion and mobility probabilities are fixed to $(\lambda, p_d) = (2\mu/\langle n \rangle, 0.1)$, where $\langle n \rangle$ is the average population per node.

reaching the steady regime where all the subpopulations are not homogeneously affected. This heterogeneous incidence of an epidemic with a local seed could be related to the previous studies about the existence of different invasion thresholds[2]. In Fig. 5.c we show the same evolution as obtained from integrating the Markovian equations. In this case, despite of the fluctuating nature of Monte Carlo dynamics, the probabilistic framework captures in a very precise way the same sequence of epidemic onsets in the transient regime and the steady pattern of infection across the patches. Given this agreement, invasion thresholds can be easily determined with the help of Markovian equations by localizing the initial infected seed in each single node and studying the minimum value of the contagion probability needed for the disease to spread to other patches.

Finally, to observe the accuracy of the Markovian equations more clearly, in Fig.5.d we show, for a few neighbourhoods, a comparison between Monte Carlo results and the Markovian results about the spatio-temporal evolution of a disease. It becomes clear that our approach is very accurate, since there is a fair agreement between theory and simulations.

6 Role of asymmetry

In this section, we study the effect of population asymmetry on the epidemic threshold. For this purpose, we are going to represent the mobility dependence of this magnitude for several values of the asymmetry α. As we can notice in Fig. 6, an increase in the population asymmetry, i.e, a decrease of α, makes the detriment zone wider. To explain this fact, we have to take into account that the observed rebound happens because the number of contacts made by the leaves residents surpass the contacts made by hub agents. This way, since asymmetry implies that a larger mobility is required to gather inside the hub the same number of agents from the leaves, the detriment zone becomes wider.

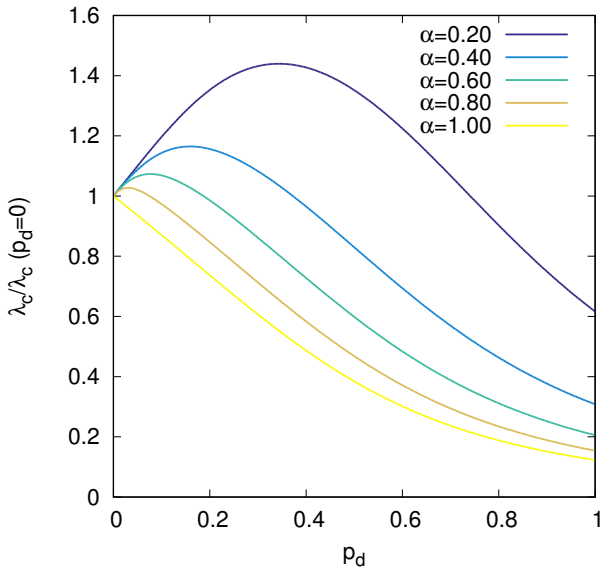

Figure 6: Mobility dependence of the epidemic threshold for several values of the population asymmetry α. The used network has $k = 10$ leaves and $\delta = 0.9$.

7 SIR model

In this section, we adapt our formalism to the case where reaction processes are governed by a SIR (Susceptible-Infected-Recovered) model. In this model, a susceptible also become infected after contacting an infected agent with probability λ. Besides, infected individuals recover with a probability μ but, unlike the SIS model, they remain in this recovered state.

Given N subpopulations, the addition of a new available compartment requires $2 \cdot N$ equations in order to characterise the spatio-temporal evolution of a disease. Specifically, assuming the same dynamical premises as in our SIS model, for each subpopulation i these two equations read:

$$\rho_i(t+1) = (1-\mu)\rho_i(t) + (1-\rho_i(t)-r_i(t))\Pi_i(t) \ , \tag{30}$$

$$r_i(t+1) = r_i(t) + \mu\rho_i(t) \ , \tag{31}$$

where $\Pi_i((t)$ is given by Eq.(2) in the main text.

8 Synthetic Networks: Random Geometric Graphs

In this section, we aim at showing the accuracy of the predictions of our model about the incidence of a disease as well as the epidemic threshold for some synthetic networks. In fact, we will consider that human flows are governed by a Random Geometry Graph (RGG), where nodes are randomly distributed on a square grid 1×1 and their interaction is constrained by geometrical distances, in such a way that a node is only connected with those situated closer than a radius R. This way, RGG have already been used to model epidemic processes where contagion only occurs among nearby humans [3]. Referring to our model, the geometrical constraints restrict human movements to places which are geographically close to their residence, what reflects a rather usual situation. Concretely, we have used a RGG network with 100 nodes and radius R=0.15. Besides, the populations inside these nodes are randomly distributed within an interval (200,2000). A representation of the network used in this section can be found in Fig.7.a.

To validate our equations, we compare their predictions about the incidence of a disease by using SIS [Eqs.(1-4) in the main text] and SIR [Eqs.30,31)] dynamics to the results obtained via Monte Carlo simulations. As we can notice in Figure 7.b and 7.c, there is a fair agreement between Monte Carlo simulations and the Markovian solution. Moreover, in order to characterise the epidemic regime of this particular network, we make use of Eq. (8) in the main text to calculate the epidemic threshold for each value of agents mobility p_d. In Figure 7.d we represent this parameter for each value of human mobility along with the fraction of infected people as a function of (p_d, λ). It is clear that our estimation of the epidemic threshold is quite accurate. Besides, we can notice that this metapopulation lies on regime II, since there is a non-monotonous epidemic detriment.

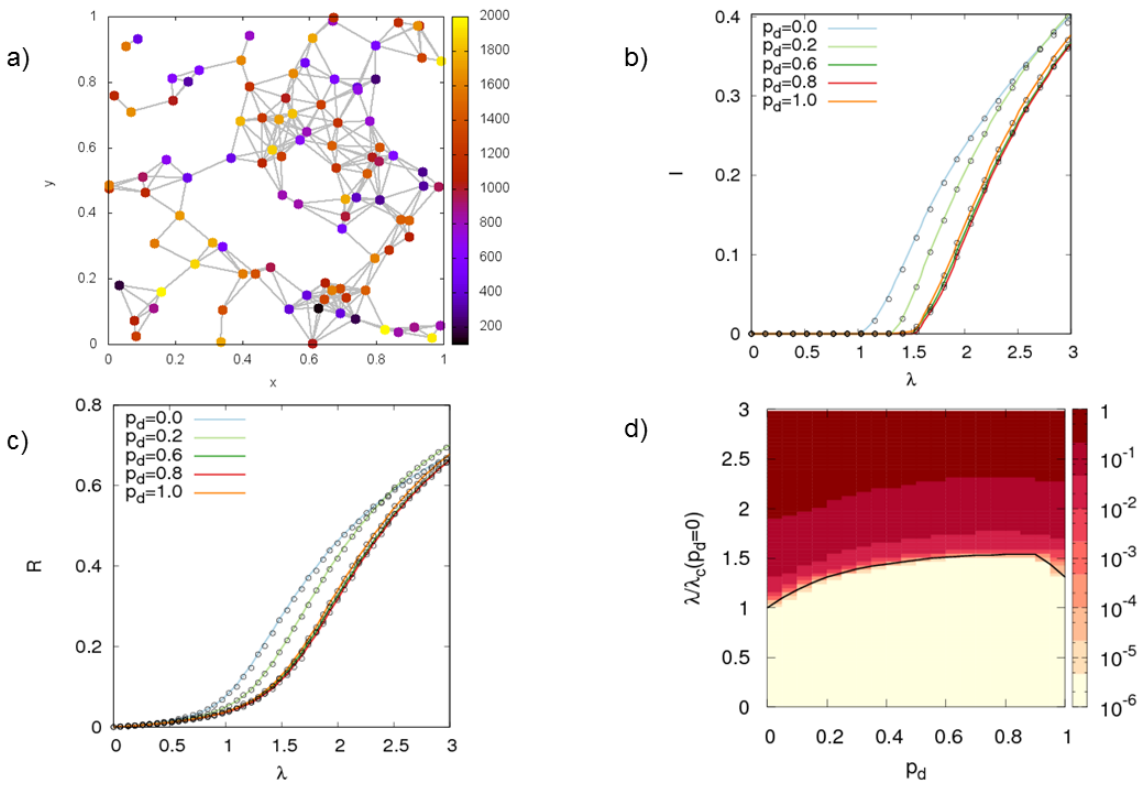

Figure 7: Panel a). RGG network of 100 nodes with R=0.15. The colour of each node denotes its population, with values ranging from 200 to 2000 inhabitants. Panels b) and c) show the incidence of a disease using SIS (b) or SIR (c) dynamics as a function of the contagion rate λ and the mobility of the agents p_d. Note that λ has been normalised by the static epidemic threshold. In both cases, solid lines denote predictions of our equations whereas dots represent results from MC simulations. This results have been obtained by averaging 20 realizations for each value of λ and p_d. In panel d), colour represents the fraction of infected individuals obtained via numerical simulations using a SIS model for each value of (λ, p_d) while black solid line represents the epidemic threshold as a function of p_d according to Eq.(8) in the main text. The recovery rate is set to $\mu = 0.2$.

References

1. Marcus, R. A. Brief comments on perturbation theory of a nonsymmetric matrix: The gf matrix. *The Journal of Physical Chemistry A* **105**, 2612–2616 (2001).

2. Colizza, V. & Vespignani, A. Invasion threshold in heterogeneous metapopulation networks. *Physical Review Letters* **99**, 148701 (2007).

3. Estrada, E., Meloni, S., Sheerin, M. & Moreno, Y. Epidemic spreading in random rectangular networks. *Phys. Rev. E* **94**, 052316 (2016).